Temperature Dependence of Neutron-Gamma Discrimination Based on Pulse Shape Discrimination Technique in a Ce:LiCaAlF_6 Scintillator

Watanabe, Kenichi
Nagoya University

Kondo, Yoshiyuki
Nagoya University

Yamazaki, Atsushi
Nagoya University

Uritani, Akira
Nagoya University

他

出版情報：IEEE transactions on nuclear science. 60 (2), pp.959-962, 2013-01-15. Institute of Electrical and Electronics Engineers(IEEE)
バージョン：

Temperature Dependence of Neutron-gamma Discrimination Based on Pulse Shape Discrimination Technique in a Ce:LiCaAlF$_6$ Scintillator

Kenichi Watanabe, Yoshiyuki Kondo, Atsushi Yamazaki, Akira Uritani, Tetsuo Iguchi, Noriaki Kawaguchi, Kentaro Fukuda, Sumito Ishidu, Takayuki Yanagida, Yutaka Fujimoto, Akira Yoshikawa

***Abstract*— LiCaAlF$_6$ scintillators are one of the attractive scintillators for neutron detection. To reduce the effect on gamma-rays, the Ce doped LiCaAlF$_6$ scintillators can discriminate the neutron and gamma-ray events based on the pulse shape discrimination technique. To apply the scintillators for the oil logging, the high temperature characteristics must be investigated. In this paper, the temperature dependence of the neutron-gamma discrimination based on pulse shape discrimination technique in the Ce:LiCaAlF$_6$ scintillator is investigated as one of the high temperature characteristics. The property of pulse shape discrimination in the Ce:LiCaAlF$_6$ has small temperature dependence ranging from 25ºC to 150ºC. We concluded that the Ce:LiCaAlF$_6$ scintillators can discriminate neutron and gamma-ray events under high temperature condition up to 150ºC.**

***Index Terms*—Neutron, scintillator, pulse shape discrimination, gamma-ray rejection, temperature dependence**

I. Introduction

NEUTRON detection technique is widely used in many fields, such as security, material science and oil well logging. For thermal neutron detection, a He-3 proportional counter has been the gold standard as a detector. Recently, the demand of He-3 counters in homeland security and neutron science applications rapidly increase but the limited He-3 supply causes the He-3 shortage problem. The alternatives to He-3 counters, therefore, have been required. Inorganic scintillators containing lithium or boron have attracted much attention for thermal neutron detection. We have developed a novel neutron scintillator Ce:LiCaAlF$_6$ as one of the alternatives to He-3 gas counters [1-4]. A Ce:LiCaAlF$_6$ scintillator has excellent properties for neutron detection such as relatively high light yield, high alpha/beta ratio, which is defined as the ratio of light outputs per unit energy for alpha particles and electrons, and compound consisting of light elements. In addition, this scintillator can discriminate neutron and gamma-ray events based on the pulse shape discrimination technique [5]. For only gamma-ray events, a scintillation pulse shape has a quite fast component with the decay time of a few nanoseconds. On the other hand, for neutron events, it has only a relatively slow component with the decay time of a few tens nanoseconds, corresponding to the emission of Ce^{3+} ions. This fast component can be applied to discriminate neutron and gamma-ray events.

Well logging is the way to make a detailed record of geologic information of drilled holes. Neutron well logging is one of the nuclear logging techniques. In this technique, a neutron source is placed into a drilled hole and the neutrons scattered by hydrogen atoms are measured. We can estimate the porosity from the difference in the scattered neutrons. The neutron logging can be one of the applications for the Ce:LiCaAlF$_6$ scintillators. In the well logging applications, the detectors must be used in high temperature condition. Therefore, to apply the scintillators for the well logging, the high temperature characteristics must be investigated. In this paper, the temperature dependence of the neutron-gamma discrimination based on pulse shape discrimination technique in the Ce:LiCaAlF$_6$ scintillator is investigated as one of the high temperature characteristics. Especially, we confirm the temperature dependence of the relative contribution of the fast component in Ce:LiCaAlF$_6$ scintillation signal.

II. Experimental Setup

Figure 1 shows the experimental setup. A Ce:LiCaAlF$_6$ scintillator with the size of 10x10x2 mm^3 was mounted on the photomultiplier tube (PMT) for high temperature applications (Hamamatsu, R1288A) with optical grease. The scintillator was covered by Teflon tapes to collect the scintillation photons. Furthermore, the scintillator and the PMT were shielded from ambient light with an aluminum foil. The bias voltage for the

Manuscript received June 1, 2012. This study is the result of “Development of high efficiency neutron scintillator for thermal and epi-thermal neutrons” carried out under the Development of Systems and Technology for Advanced Measurement and Analysis by Japan Science and Technology Agency.

K. Watanabe, Y. Kondo, A. Yamazaki, A. Uritani, T. Iguchi are with Nagoya University, Furo-cho, Chikusa-ku, Nagoya, 464-8603, Japan (phone: +81-52-789-4513; fax: +81-52-789-3843; e-mail: k-watanabe@nucl.nagoya-u.ac.jp).

N. Kawaguchi, K. Fukuda, T. Suyama are with Tokuyama Corp., Shunan city, Yamaguchi 745-8648, Japan

T. Yanagida, Y. Fujimoto, A. Yoshikawa are with Tohoku University, 2-1-1 Katahira, Aoba-ku, Sendai 980-0812, Japan

PMT was set to -1500 V. The measurement system was temperature controlled in the thermoregulated bath, or the incubator, ranging from 25°C to 150°C. We waited for more than 1.5 hours before each measurement for temperature stabilization. A moderated Cf-252 source and Co-60 source were used for thermal neutron and gamma-ray irradiations, respectively. Neutrons and gamma rays were irradiated through the view window from outside of the thermoregulated bath.

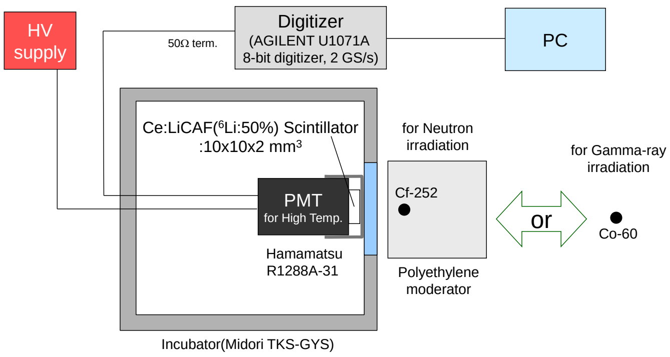

Fig. 1 Experimental setup.

The pulse shapes were recorded through the high speed digitizer (Agilent U1071A 8 bit digitizer, 2 GS/s). The input impedance of the digitizer was 50 ohms. To discriminate neutron and gamma-ray events, the pulse signal was digitally processed to extract the fast and slow components. Figure 2 shows examples of raw signal pulse shapes for gamma-ray and neutron events. Only gamma-ray events have the fast component.

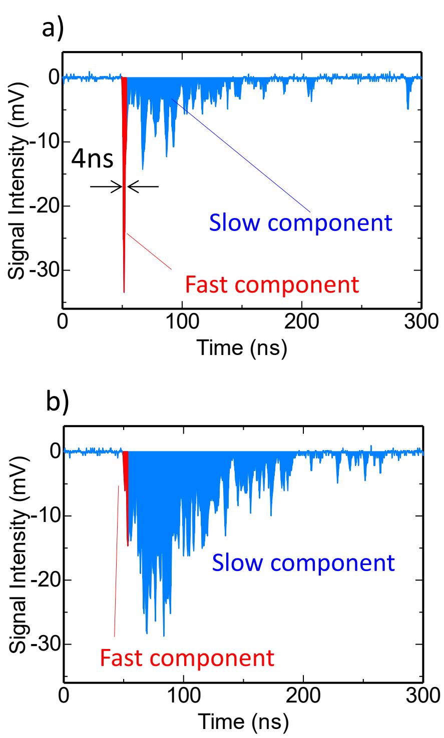

Fig. 2 Examples of raw signal pulse shapes for gamma-ray and neutron events. Areas of the region within first 4 ns of each signal were defined as the fast component. Residual areas were calculated as the slow component.

Areas of the region within first 4 ns of each signal were defined as the fast component. If there is no fast component, this region is assumed to be fast component. This 4 ns window width was not optimized. Residual areas were calculated as the slow component. An example of a two dimensional histogram between the fast and slow components is shown in Fig. 3. We can see that gamma-ray events have a relatively high contribution of the fast component compared to neutron events. Neutron and gamma-ray events were confirmed to be clearly separated.

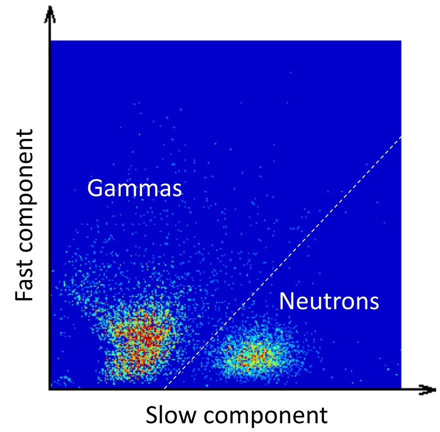

Fig. 3 An example of a two dimensional histogram between the fast and slow components for the temperature of 25°C.

The fast component might be caused by Cherenkov radiation. The Cherenkov radiation can be emitted from the PMT window. If the fast component is produced in the PMT window, the results are unique to the geometry tested in this paper. In order to generalize the temperature dependence of the scintillation characteristics in a Ce:LiCaAlF$_6$, we should confirm that the most of the fast component is not produced in the PMT window. We investigated the scintillation response using Monte Carlo simulation code EGS5[6]. In order to coincidentally output the Cherenkov radiation from the PMT window and the scintillation emission from Ce:LiCaAlF$_6$ crystal, fast electrons produced by an incident gamma-ray should run through both the scintillator and the PMT window. This probability is small because of relatively short range of fast electrons compared with the scintillator size. Additionally, in this case, the deposited energies in the scintillator and the PMT window should have a negative correlation because both of them share a given energy of fast electrons. The experimental results, however, showed a positive correlation though the fluctuation was large. This is considered to be one of the evidence that the Cherenkov radiation from the PMT window has small contribution to the fast component.

III. Results and Discussion

The temperature dependence of the two dimensional histogram between the fast and slow components was investigated to check the performance of the pulse shape discrimination over the temperatures ranging from 25°C to 150°C.

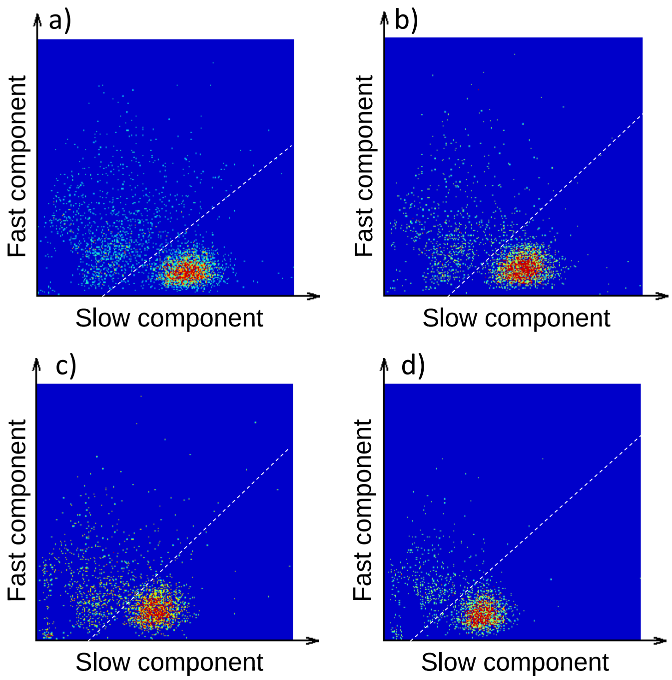

Fig. 4 The two dimensional histograms for a) 25°C, b) 50°C, c) 100°C and d) 150°C when the scintillator was irradiated by the moderated Cf-252 source.

Figure 4 shows the two dimensional histograms for various temperatures when the scintillator was irradiated by the moderated Cf-252 source. Not only neutrons but also gamma rays were detected for the moderated Cf-252 source. Over all the temperature range, neutron and gamma-ray events can be confirmed to be clearly separated in the two dimensional histograms.

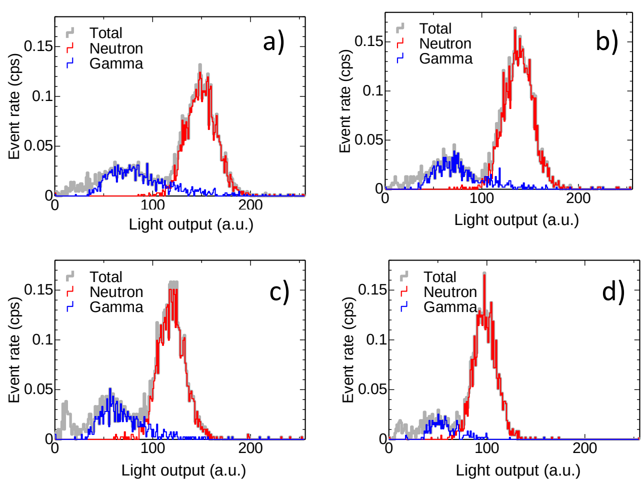

Fig. 5 The discriminated light output spectra for a) 25°C, b) 50°C, c) 100°C and d) 150°C when the scintillator was irradiated by the moderated Cf-252 source.

Since the slow component corresponds to the emission of Ce^{3+} ions, we can make the conventional light output spectra using the integral of the slow component. The conventional light output spectrum, therefore, can be obtained by integrating pixel values in the vertical direction in the two dimensional histogram. We can also distinguish between neutron and gamma-ray events by the dashed line in Fig. 4. The discriminated light output spectra for various temperatures are shown in Fig. 5.

The position of the full energy peak corresponding to neutron absorption events slightly decreases with increasing the temperature. However, the pulse shape discrimination can be carried out successfully up to 150°C.

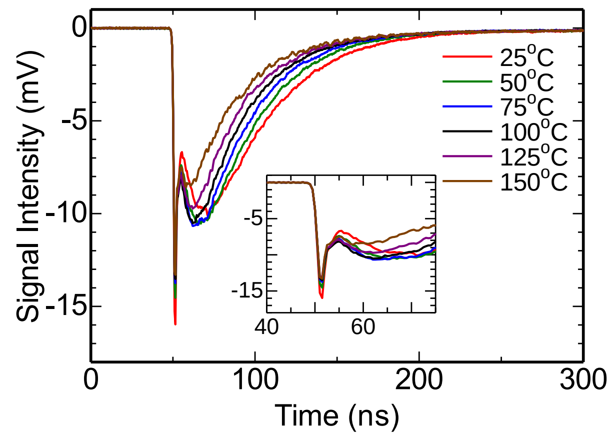

Fig. 6 The averaged pulse shapes for gamma-ray events for various temperatures.

To make a detailed discussion on the temperature dependence of the pulse shape, the averaged pulse shape was derived. For gamma-ray events, the all events obtained from a Co-60 gamma-ray source were averaged. On the other hand, for neutron events, we averaged only neutron events identified by the pulse shape discrimination in the Cf-252 experiments. Figure 6 shows the averaged pulse shapes for all events during Co-60 gamma-ray irradiation for various temperatures.

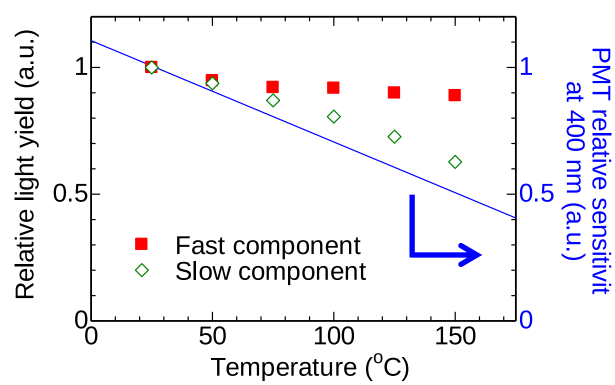

Fig. 7 The temperature dependence of the light yields of the fast and slow components.

Both of the fast and slow components depend on the temperature. Figure 7 shows the temperature dependence of the light yields of the fast and slow components. These fast and slow components were calculated from the areas of averaged signal pulses in Fig. 6. Both of the components decrease with increasing the temperature. Generally, the gain of the PMT also has the temperature dependence in which it decreases with increasing the temperature. The temperature dependence of the gain for the PMT used in these experiments was already investigated at the wavelength of 400 nm [7] and is also illustrated in Fig. 7. The temperature coefficients of quantum efficiency for a bialkali photocathode are constant less than 500 nm wavelength. The slope of decreasing the light yields of both components is shallower than that of decreasing the gain of the PMT tube. Although there m difference in the wavelengths between the investigated PMT gain and the emissions of both components, these results suggest that the light yields of both components in a Ce:$LiCaAlF_6$ scintillator might increase with the temperature. In addition, the slope of decreasing the light yield of the fast component is shallower than that of the slow component. In other words, the relative contribution of the fast component increases with the temperature. This result suggests that the pulse shape discrimination might be improved under a high temperature circumstance. However, this feature is now cancelled out due to the deterioration of the PMT gain in high temperature.

Figure 8 shows the averaged pulse shapes for neutron events corresponding to the neutron peak in the light output spectra for various temperatures. There is only the slow component but no fast component in neutron events. From these pulse shapes, we can also see the temperature dependence of the rise time and decay time. The temperature dependence of the rise time and decay time in the slow component of the Ce:$LiCaAlF_6$ scintillation is shown in Fig. 9. The decay time of the slow component slightly changes with the temperature and has a minimum value at around 100°C. On the other hand, the rise time simply decreases with increasing the temperature. This temperature dependence is larger than the PMT anode pulse rise time, which is 1.3 ns in this PMT. We consider that this dependence is produced from scintillation processes. This characteristic might be considered to arise from the charge transfer process depending on temperature.

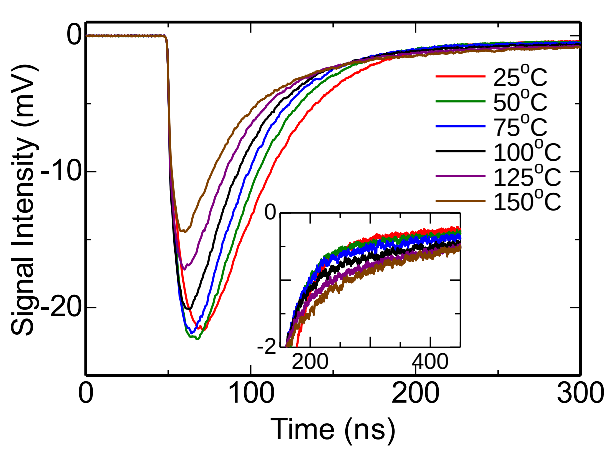

Fig. 8 The averaged pulse shapes for neutron events for various temperatures.

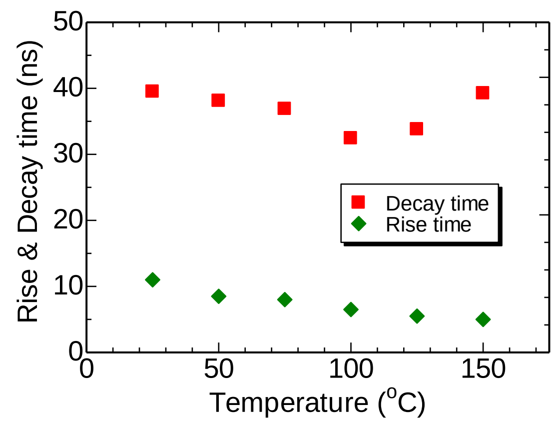

Fig. 9 The temperature dependence of the rise time and decay time in the slow component of the Ce:$LiCaAlF_6$ scintillation.

Although the fast and slow components have some properties on the temperature dependence, the fast component can occur up to the maximum tested temperature of 150°C. We, therefore, conclude that the Ce:$LiCaAlF_6$ scintillators can discriminate neutron and gamma-ray events under high temperature condition up to 150°C. Some properties on the temperature dependence obtained in this study can play an important role in understanding the origin of the fast and slow components in a Ce:$LiCaAlF_6$ scintillator.

These excellent scintillation properties in high temperature can make a Ce:$LiCaAlF_6$ scintillator available for the well logging application.

IV. Conclusion

We investigated the temperature dependence of the fast and slow components in a Ce:$LiCaAlF_6$ scintillator. The fast component occurring in gamma-ray events was confirmed to be available up to 150°C at least. Although signal intensities of the fast and slow scintillation components slightly decrease with increasing the temperature, the relative contribution of the fast component increases with the temperature. We concluded that a Ce:$LiCaAlF_6$ scintillator can discriminate neutron and gamma-ray events up to 150°C. We confirmed that a Ce:$LiCaAlF_6$ scintillator can be a promising candidate of the neutron detector for the well logging application, as alternatives to He-3 counters.

From results reported in this paper, we cannot determine the origin of the fast component. The fast component might be caused by Cherenkov radiation in a Ce:$LiCaAlF_6$ scintillator. In future work, we will try understanding the origin of the fast component in a Ce:$LiCaAlF_6$ scintillator through various investigations, such as a detailed emission spectra for neutrons and gamma rays, the temperature dependence of the relative light yields considering the temperature dependence of the PMT gain over whole wavelength range.

References

[1] A. Yoshikawa, T. Yanagida, Y. Yokota, N. Kawaguchi, S. Ishizu, K. Fukuda, T. Suyama, K.J. Kim, J. Pejchal, M. Nikl, K. Watanabe, M.

Miyake, M. Baba, K. Kamada, "Single Crystal Growth, Optical Properties and Neutron Response of Ce^{3+} Doped $LiCaAlF_6$", *IEEE Trans. Nucl. Sci.*, **56**, 2009, pp. 3796-3799.

[2] Noriaki Kawaguchi, Takayuki Yanagida, Yutaka Fujimoto, Yuui Yokota, Kei Kamada, Kentaro Fukuda, Toshihisa Suyama, Kenichi Watanabe, Atsushi Yamazaki, Valery Chani, Akira Yoshikaw, "Thermal neutron imaging with rare-earth-ion-doped $LiCaAlF_6$ scintillators and a sealed ^{252}Cf source", *Nucl. Instrum. Methods*, **A652**, 2011, pp. 351-354.

[3] Joanna Iwanowska, , , Lukasz Swiderski, Marek Moszynski, Takayuki Yanagida, Yuui Yokota, Akira Yoshikawa, Kentaro Fukuda, Noriaki Kawaguchi, Sumito Ishizu, "Thermal neutron detection with Ce^{3+} doped $LiCaAlF_6$ single crystals" , *Nucl. Instrum. Methods*, **A652**, 2011, pp. 319-322.

[4] Y. Yokota, Y. Fujimoto, T. Yanagida, H. Takahashi, M. Yonetani, K. Hayashi, I. Park, N. Kawaguchi, K. Fukuda, A. Yamaji, Y. Fukazawa, M. Nikl, A. Yoshikawa, "Crystal Growth of Na-Co-Doped Ce:$LiCaAlF_6$ Single Crystals and Their Optical, Scintillation, and Physical Properties", *Cryst. Growth Des.*, **11**, 2011, pp 4775–4779

[5] A. Yamazaki, K. Watanabe, A. Uritani, T. Iguchi, N. Kawaguchi, T. Yanagida, Y. Fujimoto, Y. Yokota, K. Kamada, K. Fukuda, T. Suyama, A. Yoshikawa, "Neutron-gamma discrimination based on pulse shape discrimination in a Ce:$LiCaAlF_6$ scintillator" , *Nucl. Instrum. Methods*, **A652**, 2011, pp. 435-438.

[6] H. Hirayama, Y. Namito, A.F. Bielajew, S.J. Wilderman and W.R. Nelson, "The EGS5 Code System", SLAC-R-730 and KEK Report 2005-8, 2005.

[7] S. Kurosawa, M. Sugiyama, T. Yanagida, Y. Yokota A. Yoshikawa, "Temperature dependence of the scintillation properties of Ce:GSO and Ce:GSOZ", *Nucl. Instrum. Methods*, A690, 2012, pp. 53-57.